A micromagnetic understanding of the post-annealing process in producing sintered Nd-Fe-B permanent magnets

1994 J. Phys.: Condens. Matter 6 6691

(http://iopscience.iop.org/0953-8984/6/33/016)

J. Phys.: Condens. Matter 6 (1994) 6691–6698. Printed in the UK

A micromagnetic understanding of the post-annealing process in producing sintered Nd–Fe–B permanent magnets

X C Kou and H Kronmüller

Max-Planck-Institut für Metallforschung, Institut für Physik, Heisenbergstraße 1, 70569 Stuttgart, Germany

Received 5 January 1994, in final form 15 April 1994

Abstract. A micromagnetic analysis of the temperature dependence of the coercivity of sintered Nd–Fe–B permanent magnets with and without post-annealing treatment has been made based on the nucleation mechanism. Two temperature ranges in which different mechanisms control the coercivity are clearly distinguishable. From the micromagnetic point of view, the post-annealing process reduces the local effective demagnetizing field ($-N_{\text{eff}}M_s$), which makes the nucleation of a reversed domain more difficult, and therefore enhances the coercivity.

1. Introduction

The liquid-phase sintering technique, which consists of pre-alloy melting, crushing, milling, magnetic field aligning and finally high-temperature sintering, is a very powerful method in producing rare-earth permanent magnets. It was found that the coercive field of the sintered magnets can be further enhanced by a post-annealing process. For sintered Nd–Fe–B permanent magnets, a post-annealing at about 880 K for about 1 h was proposed and is accepted as a necessary process in commercial production (Sagawa *et al* 1985). Investigation of the microstructure by means of optical or electron microscopy shows that after annealing at 873 K for 1 h the grain boundary and the grain surface of the $Nd_2Fe_{14}B$ phase, the main hard magnetic phase of Nd–Fe–B magnets, becomes smooth (Fidler 1987). The $Nd_2Fe_{14}B$ grains become free from crystallographic defects. However, from a theoretical point of view, it is still not yet clear why the coercive field is enhanced after the post-annealing treatment. In the present paper, we try to analyse the temperature dependence of the coercivity measured for samples after and before the post-annealing treatment. From the present analysis, we expect to find which micromagnetic parameters change during the post-annealing process. In addition, the mechanism that controls the magnetization reversal process of the Nd–Fe–B magnet will be investigated in detail.

The matrix magnetic phase in Nd–Fe–B permanent magnets is the tetragonal $Nd_2Fe_{14}B$ intermetallic compound (Herbst *et al* 1984) with a Curie temperature of 585 K (Sagawa *et al* 1985), a saturation magnetization of about 1.6 T at 300 K (Givord *et al* 1984) and a magnetocrystalline anisotropy field of 6.2 MA m^{-1} (Grössinger *et al* 1985) at 300 K. The easy magnetization direction (EMD) of $Nd_2Fe_{14}B$ is parallel to the c-axis in the temperature interval from 135 K to the Curie temperature. Below 135 K a cone spin configuration was detected. The cone angle at 4.2 K is about 30° (Givord *et al* 1984).

0953-8984/94/336691+08$19.50

2. Experimental details

The sintered Nd–Fe–B permanent magnets were prepared by the following process. First, a master alloy of composition $Nd_{15}Fe_{77}B_8$ was arc melted from the raw materials with a purity of at least 99.99 wt%, followed by mechanical crushing, ball milling (protected by alcohol) until the powder was at a mean size of 4 μm, magnetic-field aligning and finally sintering at 1323 K for 1 h under purified Ar gas. After sintering, the sample was water quenched. From microstructural investigations using optical microscopy, it was found that the $Nd_{15}Fe_{77}B_8$ magnet consists of three phases. 84% of the volume is the tetragonal $Nd_2Fe_{14}B$ matrix phase. The remaining phases are in the grain boundary: the $NdFe_4B_4$ phase and the Nd-rich Nd–Fe phase. A number of cylindrical samples with a diameter of 4 mm, and a length of 6 mm, have been cut from the sintered magnets. The intrinsic coercive field (the demagnetization field is subtracted) of these cylindrical samples has been measured from 70 to 560 K by using a vibrating sample magnetometer (VSM). This VSM is equipped with a superconducting coil, which can provide magnetic fields up to 6.4 MA m^{-1}. The magnetic field was measured by a Hall probe for which the temperature is stabilized at 293 K by alcohol. The magnetization was calibrated by pure Fe and the temperature by Ni, with a Curie temperature of 627.4 K. After the measurements, the cylindrical samples were subjected to a post-annealing treatment at 873 K for 1 h. Since the post-annealing temperature is higher than the Curie temperature of the magnets (585 K), the samples were thermally demagnetized during the post-annealing treatment. After the post-annealing treatment, the temperature dependence of the coercive field was measured. The value of the coercive field H_c is defined as the field where the irreversible susceptibility χ_{irr} reaches a maximum. The irreversible susceptibility χ_{irr} can be obtained experimentally by subtracting the reversible χ_r from the total susceptibility χ_{tot} (Kou *et al* 1993). According to this definition, the coercive field corresponds to the field where most domains reverse their magnetization under the action of the inverse applied field. It is worthwhile to note that only this definition of the coercive field gives a unique value of H_c that has a clear physical meaning for magnets in which the grains are not perfectly aligned.

3. Experimental results and intrinsic parameters of Nd–Fe–B magnets

Figure 1 shows the temperature dependence of the coercive field H_c of sintered Nd–Fe–B permanent magnets after and before the post-annealing treatment. From this measurement, it becomes evident that the magnet after the post-annealing treatment has in general higher coercive fields in the whole temperature range up to T_c. This forms the main purpose of the present paper: to understand from a micromagnetic point of view why the coercive field is enlarged after the post-annealing treatment. To do so, the intrinsic magnetic properties of $Nd_2Fe_{14}B$, e.g. the anisotropy constants, $K_1, K_2, \ldots$ and the spontaneous magnetization M_s, should be known. The values of K_1, K_2 and M_s of $Nd_{15}Fe_{77}B_8$ magnets at various temperatures corresponding to the measuring temperature of H_c were obtained by interpolating from the data as determined by Hock (1988). Hock determined the material constants, i.e. K_1, K_2 and M_s, by measuring the magnetization curves at different temperatures from 4.2 K to T_c of an $Nd_2Fe_{14}B$ single crystal. Every ten degrees a measuring point was set. This guaranteed the reliability of the data obtained by means of interpolation. A Curie temperature of 585 K for $Nd_{15}Fe_{77}B_8$ was obtained by measuring the temperature dependence of the magnetization at low applied fields (40 kA m^{-1}). The spin reorientation temperature, deduced from the measurement of the temperature dependence of the AC susceptibility for $Nd_{15}Fe_{77}B_8$, is 135 K.

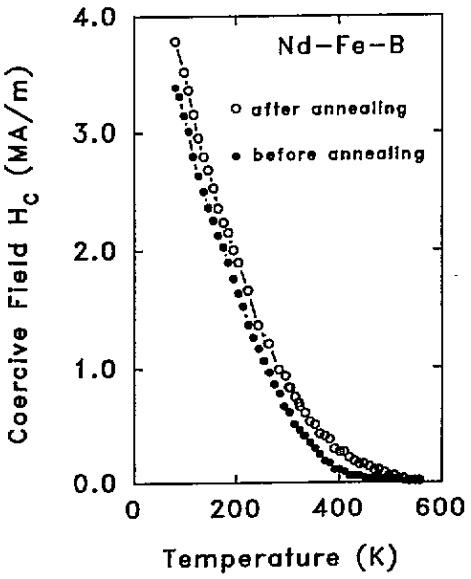

Figure 1. The temperature dependence of the coercive field H_c measured for $Nd_{15}Fe_{77}B_8$ magnets with (○) and without (●) the post-annealing treatment.

4. Micromagnetic analysis of the temperature dependence of the coercive field of $Nd_{15}Fe_{77}B_8$ permanent magnets

4.1. Theoretical background

From the micromagnetic point of view, the coercive field H_c of a permanent magnet can be expressed as (Brown 1945, Kronmüller 1966, Kronmüller *et al* 1987, Kronmüller 1991)

$$H_c = \alpha H_n - N_{eff} M_s \tag{1}$$

where H_n is the ideal nucleation field given by, e.g., $2K_1/\mu_0 M_s$ in the case $K_1 > 4K_2$. M_s is the spontaneous magnetization. α and N_{eff} are microstructural parameters. The parameter α describes the reduction of the nucleation field due to the presence of crystallographic defects in the magnetic inhomogeneous region (α_K) on the grain surface, and due to the misalignment of the grains (α_φ). Accordingly, α may be factorized, giving $\alpha = \alpha_\varphi \alpha_K$. Theoretically, both parameters, α_φ and α_K, are temperature dependent. Based on the micromagnetic theory, α_K has been calculated by Kronmüller *et al* (1987). In addition, it was deduced that the α_K value obtained can be used to predict the real mechanism that controls the coercivity (Kronmüller *et al* 1987). In the case where $\alpha_K > 0.3$, the nucleation is the leading mechanism that controls the coercivity. Otherwise, the pinning mechanism may play the leading role in determining the coercivity. The parameter N_{eff} describes the local demagnetization field, which assists the nucleation of reversed domains under the action of an applied inverse field. The values of the ideal nucleation fields, H_n, depend strongly on the value of the anisotropy constants, e.g., $K_1, K_2, \ldots$. Three regions are easily distinguished by simple calculation (Kronmüller 1985, Herzer *et al* 1986, Martinek and Kronmüller 1990):

(i) $K_1 \neq 0 \qquad K_2 = 0$

$$H_n^I = 2K_1/\mu_0 M_s \tag{2a}$$

$$\alpha_\varphi = (1/\cos\varphi)/(1 + \tan^{2/3})^{3/2} \tag{2b}$$

(ii) $K_1 > 4K_2 \qquad K_2 \neq 0$

$$H_n^{\mathrm{I}} = 2K_1/\mu_0 M_s \tag{3a}$$

$$\alpha_\varphi = [(1/\cos\varphi)/(1+\tan^{2/3}\varphi)^{3/2}](1+(2K_2/K_1)\tan^{2/3}\varphi/(1+\tan^{2/3}\varphi)) \tag{3b}$$

(iii) $-2K_2 < K_1 < 4K_2$

$$H_n^{\mathrm{II}} = \tfrac{2}{3}[2(K_1+2K_2)/\mu_0 M_s]\sqrt{(K_1+2K_2)/6K_2}. \tag{4}$$

In the third case α_φ can only be obtained by numerical calculation. From the data of anisotropy constants obtained by Hock, it follows for $Nd_2Fe_{14}B$ that in the temperature range below 180 K the condition $-2K_2 < K_1 < 4K_2$ holds, whereas in the temperature range above 180 K the condition $K_1 > 4K_2$, $K_2 \neq 0$ is applicable.

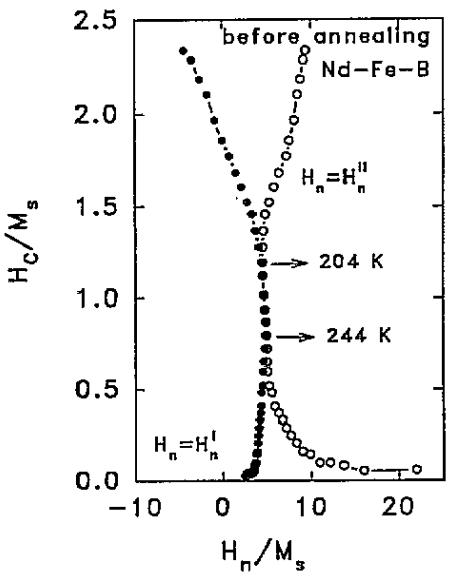

Figure 2. Plots of H_c/M_s versus H_n/M_s to test the real nucleation field at different temperatures for $Nd_{15}Fe_{77}B_8$ magnets before the post-annealing treatment. ○ represents the case where H_n^{II} is the nucleation field and ● represents the case where H_n^{I} is the nucleation field.

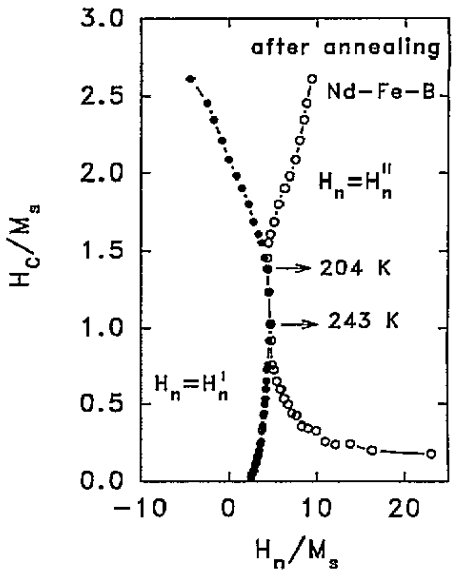

Figure 3. Plots of H_c/M_s versus H_n/M_s to test the real nucleation field at different temperatures for $Nd_{15}Fe_{77}B_8$ magnets after the post-annealing treatment. ○ represents the case where H_n^{II} is the nucleation field and ● represents the case where H_n^{I} is the nucleation field.

It is worthwhile to note that the physical meanings of H_n^{I} and H_n^{II} are rather different. In the case where H_n^{I} is the nucleation field, the magnetic moment reverses directly via expansion of reversed domains from the c-axis to the antiparallel direction as soon as the applied field is greater than H_n^{I}. There is no deviation of magnetic moments from the c-axis before reversal. On the other hand, when H_n^{II} is the nucleation field, the angle between the magnetic moment and the c-axis increases with increasing applied field in the case where the applied field is greater than $(2K_1/\mu_0 M_s)$. The complete reversal via an expansion of a nucleated reversal domain occurs when the applied field becomes greater than H_n^{II}.

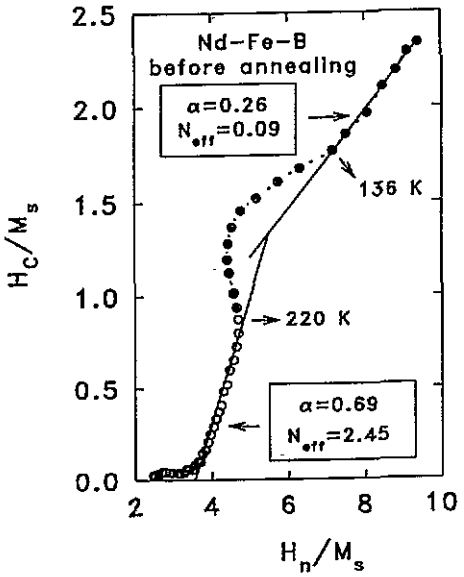

Figure 4. The least-squares linear fit of the H_c/M_s versus H_n/M_s curves at two distinguishable temperature ranges for $Nd_{15}Fe_{77}B_8$ magnets before the post-annealing treatment. At temperatures below 220 K, $H_n = H_n^{II}$ (●), whereas at temperatures above 220 K, $H_n = H_n^{I}$ (○).

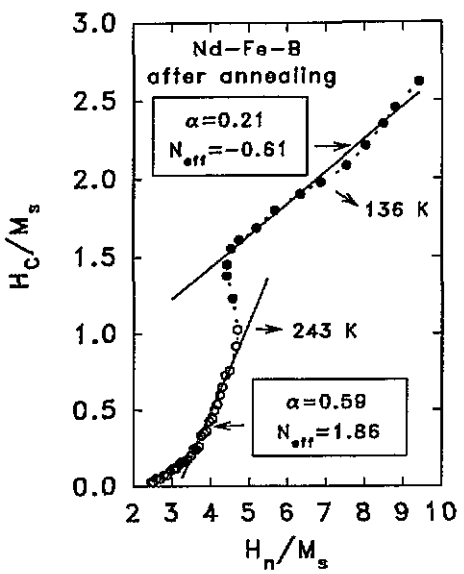

Figure 5. The least-squares linear fit of the H_c/M_s versus H_n/M_s curves at two distinguishable temperature ranges for $Nd_{15}Fe_{77}B_8$ magnets after the post-annealing treatment. At temperatures below 243 K, $H_n = H_n^{II}$ (●), whereas at temperatures above 243 K, $H_n = H_n^{I}$ (○).

4.2. Analysis based on the micromagnetic model

As discussed above, the coercive field H_c of permanent magnets can be expressed by (1) in which H_c, H_n and M_s are temperature dependent, but N_{eff} is not. Therefore, if H_c/M_s is plotted as a function of H_n/M_s at various temperatures, the existence of a linear relationship will justify the applicability of (1).

In order to clarify in which temperature range H_n^I or H_n^{II} is actually the nucleation field for an $Nd_{15}Fe_{77}B_8$ magnet, plots of H_c/M_s versus H_n^I/M_s and H_c/M_s versus H_n^{II}/M_s before and after a post-annealing treatment at various temperatures were made and are shown in figures 2 and 3. From these plots, it is evident that at temperatures lower than about 180 K, H_n^{II} is the real nucleation field, whereas at temperatures higher than about 240 K, H_n^I is the nucleation field. In the temperature range from 180 to 240 K there actually exists no difference between these two nucleation fields. These three temperature ranges can be clearly seen in figures 4 and 5. We have tried to use the least-squares linear fitting program to fit the H_c/M_s versus H_n^I/M_s and H_c/M_s versus H_n^{II}/M_s curves. Figures 4 and 5 show the results of fitted plots. It is found that this fitting for the magnets without the post-annealing treatment is only reasonable at temperatures below 136 K (where H_n^{II} is the nucleation field) and from 220 to about 400 K (where H_n^I is the nucleation field). The fitting parameters obtained are included in figure 4. For magnets after a post-annealing treatment, a linear relationship is reasonable at temperatures below 180 K (where H_n^{II} is the nucleation field) and from 243 to 420 K (where H_n^I is the nucleation field). Fitting parameters α and N_{eff}, obtained from this procedure, are shown in figure 5. From this analysis it follows that two temperature ranges can be clearly distinguished for $Nd_{15}Fe_{77}B_8$ magnets, both with and without the post-annealing treatment. It can be suggested that the mechanism which

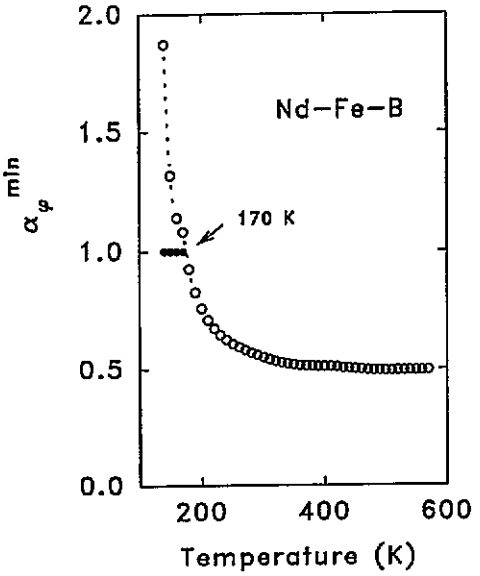

Figure 6. The temperature dependence of α_φ^{min} calculated for $Nd_{15}Fe_{77}B_8$ magnets (○) by using (3*b*) and the highest physically meaningful values below 170 K ($\alpha_\varphi^{min} = 1$) (●).

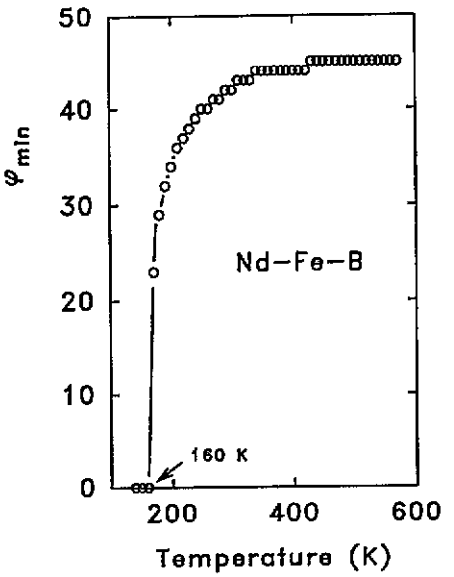

Figure 7. The temperature dependence of the angle φ_{min} where α_φ is a minimum.

controls the coercivity in these two temperature ranges is not the same. A large difference in the value of N_{eff} is evident between these two temperature ranges. In the temperature range where H_n^I is the nucleation field, the value of N_{eff} is rather large. This might imply that the magnetization reversal process in this temperature range is realized through nucleation of reversed domains which occurs preferentially in regions on the grain surface where the local effective demagnetizing field ($-N_{eff}M_s$) is the largest. On the other hand, in the temperature range where H_n^{II} is the nucleation field, the value of N_{eff} is rather small or even negative. This means that the nucleation of reversed domains in this temperature range is not enhanced due to large local effective demagnetizing fields. In addition, the fitting parameters α and N_{eff} in the temperature range where H_n^I is the nucleation field are larger for the magnets without post-annealing treatment than for the magnets with the post-annealing treatment. This fact suggests, at a first glance, that the post-annealing treatment reduces the local effective demagnetizing field. This leads to the conclusion, from a microstructural point of view that the post-annealing treatment makes the grains rounder and the grain surfaces smoother. This is in agreement with the microstructural investigation of $Nd_{15}Fe_{77}B_8$ grains by optical as well as electronic microscopes (Fidler 1987).

All the discussion above is made under the assumption that the easy magnetization direction (the *c*-axis for the $Nd_{15}Fe_{77}B_8$ magnet) of all grains is perfectly aligned and is antiparallel to the inversely applied field. However, in a real magnet a distribution of the alignment exists. The nucleation field differs therefore from one misaligned grain to another. In this case, the coercive field of the bulk magnet is determined by those grains that have the minimum nucleation field ($H_n^{min} = \alpha_\varphi^{min} H_n$). For a given temperature, the angular dependence of α_φ can be calculated from (2*b*) or (3*b*) in the case where H_n^I is the nucleation field. Figure 6 shows the temperature dependence of α_φ^{min} calculated for $Nd_{15}Fe_{77}B_8$ magnets. It is of interest to note that the angle where α_φ achieves the minimum

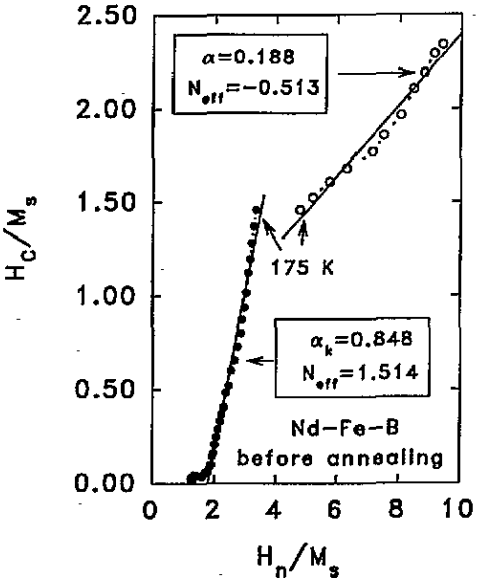

Figure 8. The linear least-squares fit of the H_c/M_s versus H_n/M_s curves at two distinguishable temperature ranges for $Nd_{15}Fe_{77}B_8$ magnets before the post-annealing treatment. At temperatures below 175 K, $H_n = H_n^{II}$ (○), whereas at temperatures above 175 K, $H_n = H_n^{min} = \alpha_\varphi^{min} H_n^I$ (●).

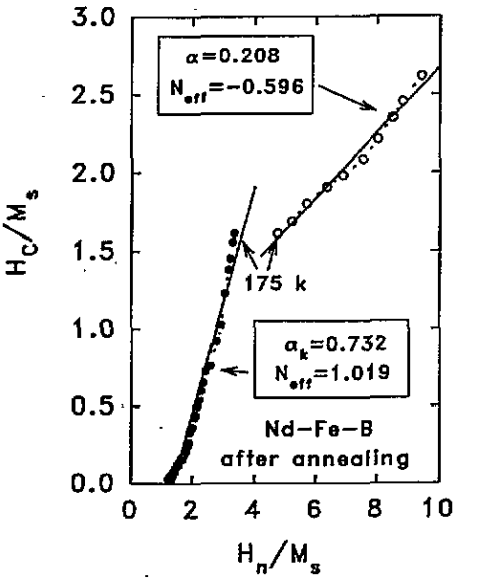

Figure 9. The linear least-squares fit of the H_c/M_s versus H_n/M_s curves at two distinguishable temperature ranges for $Nd_{15}Fe_{77}B_8$ magnets after the post-annealing treatment. At temperatures below 175 K, $H_n = H_n^{II}$ (○), whereas at temperatures above 175 K, $H_n = H_n^{min} = \alpha_\varphi^{min} H_n^I$ (●).

depends strongly on the temperature as shown in figure 7. Figures 8 and 9 show the plots of H_c/M_s versus H_n^{min}/M_s for $Nd_{15}Fe_{77}B_8$ magnets before and after a post-annealing treatment, respectively. Comparing figures 8 and 9 to figures 4 and 5, respectively, shows that the temperature range where the linear relationship between H_c/M_s and H_n^{min}/M_s holds is larger than that where the linear relationship between H_c/M_s and H_n^I/M_s is valid, for magnets both with and without the post-annealing treatment. This suggests that the misalignment of grains has a large effect on the coercive field in sintered magnets. A least-squares linear fitting program was used to fit the H_c/M_s versus H_n^{min}/M_s curve at temperatures above 175 K. The fitting parameters, α_K and N_{eff}, are included in the corresponding figures. Compared to the $Nd_{15}Fe_{77}B_8$ magnet with the post-annealing treatment, the $Nd_{15}Fe_{77}B_8$ magnet without the post-annealing treatment in the temperature range above 175 K has larger values of α_K and N_{eff}. From a micromagnetic point of view, a larger value of α_K results in smaller inhomogeneous regions on the grain surface and in turn leads to less opportunity for the nucleation of the reversed domain. This means the larger value of α_K leads to the enhancement of the coercive field. On the other hand, an enhanced value of N_{eff} results in a larger local effective stray field, which assists the nucleation of reversed domains and hence reduces the coercive field. The post-annealing treatment leads to the reduction of the values of α_K and N_{eff}. This corresponds to widening the inhomogeneous region on the grain surface. A reduction of α_K leads to the reduction of the coercive field, whereas a reduction of N_{eff} leads to lower local effective stray field, which impedes the nucleation of reversed domains and hence enhances the coercive field. From the above discussion it follows that the micromagnetic parameters, α_K and N_{eff} influence the changes in coercive field during the post-annealing process in opposite ways. The question now

arises of which influences play the leading role during the post-annealing process with respect to an enhancement of the reduction of H_c. A calculation at 300 K is helpful in understanding this question. The enhancement of the coercive field due to the reduction of N_{eff} during the post-annealing process is $M_s((-N_{eff}^{aa}) - (-N_{eff}^{ba})) = 0.63$ MA m^{-1} at 300 K, whereas the reduction of coercive field due to the increase of α_K during the post-annealing process is $\alpha_\varphi H_n^I(\alpha_K^{aa} - \alpha_K^{ba}) = -0.35$ MA m^{-1} at 300 K. Here aa represents the case after the post-annealing treatment and ba that before the post-annealing treatment. It becomes evident that the enhancement of the coercive field of the sintered Nd–Fe–B permanent magnet during the post-annealing process is mainly due to the reduction of the effective demagnetization field. This means, from the micromagnetic point of view, the grain surfaces of the sintered Nd–Fe–B permanent magnet become smoother and rounder after post-annealing treatment. This conclusion, from the micromagnetic point of view, is in good agreement with the investigation of the microstructure by means of optical or electronic microscopy (Fidler 1987), where rounder grains and smoother grain boundaries were found after the post-annealing treatment.

Finally, it is noted that it seems impossible to use the same model to describe the temperature dependence of the coercive field of sintered Nd–Fe–B permanent magnets over the whole magnetically ordered temperature range. Different mechanisms must be proposed. Note also that Hu *et al* (1993) have tried to analyse the temperature dependence of the coercivity of sintered Nd–Fe–B permanent magnets in three temperature ranges. This work is still in progress.

Acknowledgments

The authors thank Dr W J Qiang for providing the sintered magnets and Sun Li, G Rieger, J Bauer, I Kleinschroth and Dr M Seeger for fruitful discussions and friendly help.

References

Brown W F Jr 1945 *Rev. Mod. Phys.* **17** 15
Fidler J 1987 *IEEE Trans. Magn.* **MAG-23** 2106
Givord D, Li H S and Perrier de la Bâthie P 1984 *Solid State Commun.* **51** 857
Grössinger R, Sun X K, Eibler R, Buschow H K J and Kirchmayr H R 1985 *J. Physique Coll.* **46** C6 221
Herbst J F, Croat J J, Pinkerton F E and Yelon W B 1984 *Phys. Rev.* B **29** 4176
Herzer G, Fernengel W and Adler E 1986 *J. Magn. Magn. Mater.* **58** 48
Hock S 1988 *Thesis* University of Stuttgart
Hu J, Kou X C and Kronmüller H 1993 *Phys. Status Solidi* a **138** K41
Kou X C, Qiang W J, Kronmüller H and Schultz L 1993 *J. Appl. Phys.* **74** 6791
Kronmüller H 1966 *Magnetisierungskurve der Ferromagnetika (Moderne Probleme der Metallphysik)* ed A Seeger (Berlin: Springer) p 24
—— 1985 *Phys. Status Solidi* b **130** 197
—— 1991 *Supermagnets, Hard Magnetic Materials* ed G J Long and F Grandjean (Deventer: Kluwer) ch 19 p 461
Kronmüller H, Durst K-D and Martinek G 1987 *J. Magn. Magn. Mater.* **69** 149
Martinek G and Kronmüller H 1990 *J. Magn. Magn. Mater.* **86** 177
Sagawa M, Fujimura S, Yamamoto H, Matsuura Y and Hirosawa S 1985 *J. Appl. Phys.* **57** 4096